JOURNAL OF GUIDANCE, CONTROL, AND DYNAMICS
Vol. 37, No. 5, September–October 2014

Engineering Notes

Quaternion-Based Coordinates for Nonsingular Modeling of High-Inclination Orbital Transfer

Paola Libraro,* N. Jeremy Kasdin,† and Edgar Y. Choueiri‡
Princeton University, Princeton, New Jersey 08544
and
Atri Dutta§
Wichita State University, Wichita, Kansas 67260

DOI: 10.2514/1.G000613

Nomenclature

c	=	characteristic constant for satellite propulsion system, m/s
F_1, F_2, F_3	=	thrust components in reference frame $(\hat{\boldsymbol{b}}_1, \hat{\boldsymbol{b}}_2, \hat{\boldsymbol{e}}_r)$, N
I_{sp}	=	specific impulse of the thruster, s
m	=	mass of the spacecraft, kg
$\boldsymbol{q}$	=	quaternion vector of components $q_1(t)$, $q_2(t)$, $q_3(t)$, and $q_4(t)$
r	=	radial position, km
T	=	thrust magnitude, N
T_{max}	=	maximum thrust, N
t	=	time variable, s
t_f	=	final time, s
$\boldsymbol{u}$	=	control vector
u, v, w	=	velocity vector components, m/s
$\boldsymbol{x}$	=	state vector
α, β	=	thrust direction angles in reference frame $(\hat{\boldsymbol{e}}_\phi, \hat{\boldsymbol{e}}_\theta, \hat{\boldsymbol{e}}_r)$, rad
θ, ϕ, ψ	=	Euler angles, rad
ω_1, ω_2, ω_3	=	angular velocity vector components, rad/s

I. Introduction

RECENTLY, the potential of electric propulsion (EP) for orbit transfer of scientific or commercial satellites has begun to be recognized both by satellite manufacturers and providers [1,2]. The increasing interest in EP to perform primary maneuvers for geocentric missions (until now, under the domain of chemical propulsion) is first motivated by the potential mass savings this technology enables due to the high I_{sp} and more efficient propellant management compared to conventional chemical rockets. This mass saving directly translates into more room for payload or the possibility of using smaller (and thus less expensive) launch vehicles.

Received 10 March 2014; revision received 5 May 2014; accepted for publication 8 May 2014; published online 12 August 2014.

*Ph.D. Student, Mechanical and Aerospace Engineering. Student Member AIAA.

†Professor, Mechanical and Aerospace Engineering. Associate Fellow AIAA.

‡Professor, Mechanical and Aerospace Engineering. Fellow AIAA.

§Assistant Professor, Aerospace Engineering. Member AIAA.

The challenges associated with low-thrust orbit raising using EP come from the long transfer times; the need for continuous, and relatively high, power; and the resulting long exposure to radiation from the Van Allen belts. In [3–5], an optimization tool to determine orbit-raising trajectories to geostationary Earth orbit (GEO) for all-electric telecommunication satellites, which minimizes both time of flight and radiation damage on the solar arrays, was developed. However, the range of possible orbits studied in such previous work was constrained by the limitations of the dynamic model. In those optimizations, the equations of motion were written using spherical coordinates in a spherical frame, which are a more robust formulation than using Cartesian coordinates. [6] However, this choice of coordinate system also introduces singularities at 90 deg inclination, putting an upper limit on the inclination of the injection orbit options that can be considered. There are two reasons for considering high-inclination injection orbits. Because of the figure-eight form of the cross section of the Van Allen belt, high-inclination injection orbits can minimize the incidence of radiation during the initial part of the transfer (when the spacecraft moves through the inner hazardous part of the Van Allen belt). Second, having longer solar exposure for the solar arrays, resulting from a sun-synchronous orbit for example, reduces the eclipse duration, and consequently the onboard energy storage system requirement and its associated mass penalty for continuous thrust.

Although a globally nonsingular description of the satellite dynamics could be found by returning to Cartesian coordinates, it is known that the rapid variation along with switching signs of Cartesian coordinates makes numerical optimization extremely sensitive. Several variations of parameters approaches (using Gauss-like planetary equations) have been proposed using alternative nonsingular orbital elements [6–9]. However, these approaches are numerically complex, complicating an optimization scheme, and result in an osculating description of the trajectory. The goal of this Note is to use a coordinate description rather than an osculating parametric description. Thus, it will be presented in the following pages the definition, implementation, and validation of an alternative set of globally nonsingular equations of motion based on quaternions that can be used in low-thrust models to overcome the limits of previous formulations.

Although quaternions are commonly used as a globally nonsingular and numerically robust set of coordinates for satellite attitude dynamics [10–15], and as a replacement for the angular orbital elements in an osculating description [7] to remove singularities, they have not been used as coordinates for position in the two-body problem. Described here is a formulation of Newton's second law for the position of a satellite in terms of radial distance and quaternions that can be used in a direct optimization scheme. Although the specific application considered to test the new set of equations is the transfer from a high-inclination orbit to GEO, the approach is applicable to any general orbital transfer problem.

In the following sections of the Note, the new coordinates, their constraints, and the equations of motion have been derived. The new equations are tested by integrating them in MATLAB and comparing the final result to the Cartesian case. Moreover, the MATLAB integration of the new set of equations has the equally important goal of providing approximate upper bounds on the transfer time and fuel expenditure of a specific orbital transfer.

The goal of this Note is to present the new coordinates and equations of motion, and to validate the formulation on the low-thrust orbit-raising problem. It will be in the scope of a future paper formulating a minimum-time optimization problem and comparing the results to the previous approach using spherical coordinates [3]. Then, it will possible to use the optimization model to design minimum-time and minimum-radiation transfers from high-inclination injection orbits.

II. Equations of Motion

In this section, the equations of motion for a single particle in orbit about the Earth are presented. After a review of the previous formulation using spherical coordinates, it is shown how singularities can be removed by introducing quaternions to replace the usual two angle coordinates. In addition to removing the singularity, this formulation has the added benefit of keeping all variables of order unity.

A. Previous Formulation

The standard modeling approach for the orbit-raising problem uses spherical coordinates, $(r, \theta, \phi)_{\mathcal{I}}$, to describe the trajectories, where r is the radial distance from the origin of the inertial frame $\mathcal{I}$; θ is the azimuthal angle; and ϕ is the colatitude. These are depicted in Fig. 1. The state vector components, $\boldsymbol{x}(t) = [r(t), \theta(t), \phi(t), u(t), v(t), w(t), m(t)]$, then consist of the position, velocity, and mass of the satellite at any time t. The vector position of the object in the inertial frame in terms of the three spherical coordinates is given by

$$\boldsymbol{r} = r \cos\theta \sin\phi \boldsymbol{e}_x + r \sin\theta \sin\phi \boldsymbol{e}_y + r \cos\phi \boldsymbol{e}_z \tag{1}$$

The spherical reference frame $\mathcal{B}_s$, shown in Fig. 1, has the first axis, defined by the unit vector $\boldsymbol{e}_\phi$, pointed south; the third axis, denoted by $\boldsymbol{e}_r$, pointed in the radial direction; and the second, denoted by the unit vector $\boldsymbol{e}_\theta$, completing the right-handed set and pointed east. This frame can be obtained from the inertial frame via three-axis and two-axis rotations by the spherical angles θ and ϕ [16]. The resulting direction-cosine matrix (DCM) between the spherical frame and inertial frame is given by

$$^{\mathcal{B}_s}C^{\mathcal{I}} = \begin{bmatrix} \cos\theta\cos\phi & \sin\theta\cos\phi & -\sin\phi \\ -\sin\theta & \cos\theta & 0 \\ \cos\theta\sin\phi & \sin\theta\sin\phi & \cos\phi \end{bmatrix} \tag{2}$$

It is easily confirmed that the position vector in $\mathcal{B}_s$, $\boldsymbol{r} = r\boldsymbol{e}_r$, when multiplied by the transpose of the DCM in Eq. (2), gives the inertial position vector in Eq. (1). Similarly, the angular velocity vector for the 3-2 rotation is given by

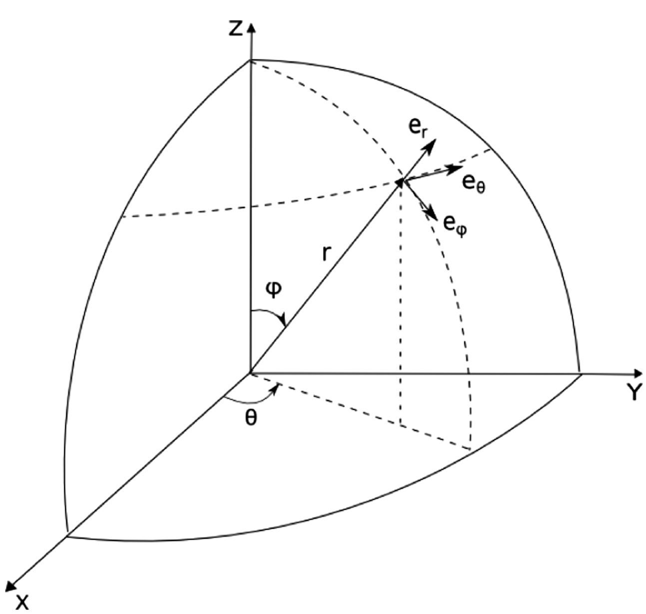

Fig. 1 Earth-centered inertial frame, spherical reference frame, and spherical coordinates $r(t)$, $\theta(t)$, and $\phi(t)$.

$$^{\mathcal{I}}\boldsymbol{\omega}^{\mathcal{B}_s} = -\dot{\theta}\sin\phi\boldsymbol{e}_\phi + \dot{\phi}\boldsymbol{e}_\theta + \dot{\theta}\cos\phi\boldsymbol{e}_r \tag{3}$$

The inertial velocity of the satellite is given by the inertial derivative of the position

$$\boldsymbol{v} = \frac{^{\mathcal{I}}\mathrm{d}}{\mathrm{d}t}\boldsymbol{r} = \frac{^{\mathcal{B}_s}\mathrm{d}}{\mathrm{d}t}\boldsymbol{r} + {}^{\mathcal{I}}\boldsymbol{\omega}^{\mathcal{B}_s} \times \boldsymbol{r} \tag{4}$$

which results in the expression

$$\boldsymbol{v} = r\dot{\phi}\boldsymbol{e}_\phi + r\dot{\theta}\sin\phi\boldsymbol{e}_\theta + \dot{r}\boldsymbol{e}_r \tag{5}$$

The generalized speeds $u(t)$, $v(t)$, and $w(t)$ are used for the equations of motion. The velocity vector can be written in terms of these speeds as follows:

$$\boldsymbol{v} = u(t)\boldsymbol{e}_\phi + v(t)\boldsymbol{e}_\theta + w(t)\boldsymbol{e}_r \tag{6}$$

where the component magnitudes $u(t)$, $v(t)$, and $w(t)$ can be written in terms of $r(t)$, $\theta(t)$, and $\phi(t)$; and their first time derivatives can be written as

$$u = r\dot{\phi}, \qquad v = r\dot{\theta}\sin\phi, \qquad w = \dot{r} \tag{7}$$

The acceleration is then given by the inertial derivative of the velocity

$$\boldsymbol{a} = \dot{u}\boldsymbol{e}_\phi + \dot{v}\boldsymbol{e}_\theta + \dot{w}\boldsymbol{e}_r + {}^{\mathcal{I}}\boldsymbol{\omega}^{\mathcal{B}_s} \times \boldsymbol{v} \tag{8}$$

which results in

$$\boldsymbol{a} = \left(\dot{u} + \frac{uw - v^2\cot\phi}{r}\right)\boldsymbol{e}_\phi + \left(\dot{v} + \frac{vw + uv\cot\phi}{r}\right)\boldsymbol{e}_\theta + \left(\dot{w} - \frac{u^2 + v^2}{r}\right)\boldsymbol{e}_r \tag{9}$$

The resulting equations of motion in state-space form are then

$$\dot{\phi} = \frac{u}{r} \tag{10a}$$

$$\dot{\theta} = \frac{v}{r\sin\phi} \tag{10b}$$

$$\dot{r} = w \tag{10c}$$

$$\dot{u} = \frac{-uw + v^2\cot\phi}{r} + \frac{T}{m}\sin\beta \tag{10d}$$

$$\dot{v} = -\frac{vw + uv\cot\phi}{r} + \frac{T}{m}\sin\alpha\cos\beta \tag{10e}$$

$$\dot{w} = \frac{u^2 + v^2}{r} - \frac{\mu}{r^2} + \frac{T}{m}\cos\alpha\cos\beta \tag{10f}$$

$$\dot{m} = -\frac{T}{c} \tag{10g}$$

The control vector $\boldsymbol{u}(t) = (T, \alpha, \beta)$ includes the thrust magnitude T and two angles describing the orientation of the thrust vector in the spherical frame. The angle between the unit vector $\boldsymbol{e}_r$ and the thrust vector projection on the plane defined by the unit vectors $\boldsymbol{e}_r$ and $\boldsymbol{e}_\theta$ is given by α. The direction of the thrust vector is completed by β, which is the angle the thrust vector makes with the plane defined by $\boldsymbol{e}_r$ and

$\boldsymbol{e}_\theta$. Although this formulation using spherical coordinates has proved to work well when considering injection orbits at low inclinations, it becomes singular when the latitude approaches 90 deg. For this reason, it is considered, replacing the two spherical angles by quaternions.

B. Quaternion for Position

To investigate high-inclination orbits, one needs to provide a nonsingular formulation of the equations of motion. Two main alternatives are available for this purpose: applying variation of parameters [17] or changing coordinate system. Variation of parameters in terms of orbital elements has been used in previous studies of orbital transfer [8,9] in which the final orbit (GEO in the case of most communication satellites) is singular due to zero inclination and zero eccentricity. Hence, the optimal trajectory achieved by these methods is feasible only in an approximate sense because the final orbit achieved is not exactly GEO. Moreover, the orbital elements describe only a set of osculating orbits (at each instant of time) that do not necessarily coincide with the exact low-thrust trajectory. Although, in the case of the equinoctial elements, the singularities can be removed from the equations, the resulting equations are still only osculating.

There are two possible alternative coordinate systems one might consider to remove the singularity, Cartesian, and quaternions. Although Cartesian coordinates result in nonsingular equations of motion, they have the drawback of fast variations with frequent switching of signs during the transfer, thus making the optimization process numerically sensitive with respect to the choice of initial guess [6]. On the other hand, quaternions are bounded between 0 and 1, making them numerically robust and avoiding at the same time any singularity. This advantage comes at the cost of the introduction of two new constraint equations.

For the new formulation, the same 3-2-3 rotation between the inertial frame and spherical frame can be applied, only now assuming that ψ is nonzero (the final rotation about the $\boldsymbol{e}_r$ axis); the new frame will be called the quaternion frame $\mathcal{B}_q$ and defined by the unit vectors $\boldsymbol{b}_1$, $\boldsymbol{b}_2$, and $\boldsymbol{b}_3 = \boldsymbol{e}_r$. The added arbitrary angular coordinate ψ will be accounted for by an added constraint later in the development. The resulting direction-cosine matrix between the inertial and quaternion frames is

$$ {}^{\mathcal{B}_q}C^{\mathcal{I}} = \begin{pmatrix} \cos\theta\cos\phi\cos\psi - \sin\theta\sin\psi & \sin\theta\cos\phi\cos\psi + \cos\theta\sin\psi & -\sin\phi\cos\psi \\ -\cos\theta\cos\phi\sin\psi - \sin\theta\cos\psi & -\sin\theta\cos\phi\sin\psi + \cos\theta\cos\psi & \sin\phi\sin\psi \\ \cos\theta\sin\phi & \sin\theta\sin\phi & \cos\phi \end{pmatrix} \tag{11} $$

One approach to writing the direction-cosine matrix in terms of quaternions is to first rewrite it in terms of the eigenaxis $\boldsymbol{e} = [e_1, e_2, e_3]^T$ and rotation angle ξ using Euler's theorem:

$$ {}^{\mathcal{B}_q}C^{\mathcal{I}} = \begin{pmatrix} c\xi + e_1^2(1-c\xi) & e_1e_2(1-c\xi) + e_3\sin\xi & e_1e_3(1-c\xi) - e_2s\xi \\ e_2e_1(1-c\xi) - e_3s\xi & c\xi + e_2^2(1-c\xi) & e_2e_3(1-c\xi) + e_1s\xi \\ e_3e_1(1-c\xi) + e_2s\xi & e_3e_2(1-c\xi) - e_1s\xi & c\xi + e_3^2(1-c\xi) \end{pmatrix} \tag{12} $$

where $c\xi \equiv \cos\xi$ and $s\xi \equiv \sin\xi$.

The quaternions (or Euler parameters) are directly related to the components of the eigenaxis $\boldsymbol{e}$ and to the rotation angle ξ through the relationships

$$ q_1 = e_1\sin(\xi/2) \tag{13a} $$

$$ q_2 = e_2\sin(\xi/2) \tag{13b} $$

$$ q_3 = e_3\sin(\xi/2) \tag{13c} $$

$$ q_4 = \cos(\xi/2) \tag{13d} $$

Substituting the expressions in Eqs. (13a–13d) into Eq. (12), the direction-cosine matrix in terms of quaternions can be found:

$$ {}^{\mathcal{B}_q}C^{\mathcal{I}} = \begin{pmatrix} 1-2(q_2^2+q_3^2) & 2(q_1q_2+q_3q_4) & 2(q_1q_3-q_2q_4) \\ 2(q_1q_2-q_3q_4) & 1-2(q_1^2+q_3^2) & 2(q_2q_3+q_1q_4) \\ 2(q_1q_3+q_2q_4) & 2(q_2q_3-q_1q_4) & 1-2(q_1^2+q_2^2) \end{pmatrix} \tag{14} $$

Equating the matrix in Eq. (11) to the matrix in Eq. (14) term by term and going through some algebra, an explicit expression for the quaternions q_1, q_2, q_3, and q_4 in terms of θ, ϕ, and ψ can be derived:

$$ q_1 = \frac{\sin\phi}{4q_4}(\sin\psi - \sin\theta) \tag{15a} $$

$$ q_2 = \frac{\sin\phi}{4q_4}(\cos\psi + \cos\theta) \tag{15b} $$

$$ q_3 = \frac{(1+\cos\phi)}{4q_4}(\cos\theta\sin\psi + \sin\theta\cos\psi) \tag{15c} $$

$$ q_4 = \frac{1}{2}[(1+\cos\phi)(1+\cos\theta\cos\psi - \sin\theta\sin\psi)]^{1/2} \tag{15d} $$

Perhaps more usefully, the inverse of Eqs. (15a–15d) provides the Euler angles in terms of the quaternions:

$$ \phi = \cos^{-1}[1 - 2(q_1^2+q_2^2)] \tag{16a} $$

$$ \theta = \sin^{-1}\left(\frac{(q_2q_3 - q_1q_4)}{(q_1^2+q_2^2)(1/(q_1^2+q_2^2)-1)^{1/2}}\right) \tag{16b} $$

$$ \psi = \sin^{-1}\left(\frac{(q_2q_3 + q_1q_4)}{(q_1^2+q_2^2)(1/(q_1^2+q_2^2)-1)^{1/2}}\right) \tag{16c} $$

As usual, the quaternions satisfy the unit norm constraint

$$ q_1^2 + q_2^2 + q_3^2 + q_4^2 = 1 \tag{17} $$

which accounts for the added fourth coordinate to replace the three angles. Of course, only two angles and distance are needed for the three degrees of translational freedom. The second constraint will come from the equations of motion.

Given the quaternions and radial distance r, the direction-cosine matrix in Eq. (14) can be used to reexpress the position vector from Eq. (1) in the inertial frame, but now in terms of quaternions

$$\boldsymbol{r} = 2r(q_1q_3 + q_2q_4)\boldsymbol{e}_x + 2r(q_2q_3 - q_1q_4)\boldsymbol{e}_y + r(1 - 2(q_1^2 + q_2^2))\boldsymbol{e}_z \tag{18}$$

C. Equations of Motion

To find the equations of motion, one can begin by writing the general vector expressions of position, velocity, and acceleration expressed as derivatives in the rotating quaternion frame:

$$\boldsymbol{r} = r\boldsymbol{e}_r \tag{19a}$$

$$\boldsymbol{v} = \dot{r}\boldsymbol{e}_r + r^{\mathcal{I}}\boldsymbol{\omega}^{\mathcal{B}_q} \times \boldsymbol{e}_r \tag{19b}$$

$$\boldsymbol{a} = \ddot{r}\boldsymbol{e}_r + 2\dot{r}^{\mathcal{I}}\boldsymbol{\omega}^{\mathcal{B}_q} \times \boldsymbol{e}_r + r^{\mathcal{I}}\dot{\boldsymbol{\omega}}^{\mathcal{B}_q} \times \boldsymbol{e}_r + r^{\mathcal{I}}\boldsymbol{\omega}^{\mathcal{B}_q} \times {}^{\mathcal{I}}\boldsymbol{\omega}^{\mathcal{B}_q} \times \boldsymbol{e}_r \tag{19c}$$

where ${}^{\mathcal{I}}\boldsymbol{\omega}^{\mathcal{B}_q} = [\omega_1, \omega_2, \omega_3]^T$ is the angular velocity vector describing the motion of the quaternion frame in the inertial frame expressed as components in the quaternion frame. Unlike in the development of the equations of motion in spherical coordinates, where there were three generalized speeds (u, v, and w), here, there are four ($\dot{r} = w$, ω_1, ω_2, and ω_3). A second constraint thus needs to be introduced to maintain three equations in three coordinates for the three degrees of freedom by setting ω_3 identically to zero so that ${}^{\mathcal{I}}\boldsymbol{\omega}^{\mathcal{B}_q} = \omega_1\boldsymbol{b}_1 + \omega_2\boldsymbol{b}_2$. Doing so results in the velocity and acceleration components

$$\boldsymbol{v} = r\omega_2\boldsymbol{b}_1 - r\omega_1\boldsymbol{b}_2 + \dot{r}\boldsymbol{e}_r \tag{20}$$

$$\boldsymbol{a} = (r\dot{\omega}_2 + 2\dot{r}\omega_2)\boldsymbol{b}_1 - (r\dot{\omega}_1 + 2\dot{r}\omega_1)\boldsymbol{b}_2 + (\ddot{r} - r(\omega_1^2 + \omega_2^2))\boldsymbol{e}_r \tag{21}$$

Note that the direction-cosine matrix in Eq. (14) can be used to transform these into components in the inertial frame given the instantaneous values of the quaternions.

The thrust vector as components in the quaternion frame is given by $\boldsymbol{F} = F_1\boldsymbol{b}_1 + F_2\boldsymbol{b}_2 + F_r\boldsymbol{e}_r$. Setting the acceleration equal to the thrust force results in the three scalar equations of motion:

$$\dot{\omega}_2 = -\frac{2\dot{r}}{r}\omega_2 + \frac{F_1}{mr} \tag{22a}$$

$$\dot{\omega}_1 = -\frac{2\dot{r}}{r}\omega_1 - \frac{F_2}{mr} \tag{22b}$$

$$\dot{w} = r(\omega_1^2 + \omega_2^2) - \frac{\mu}{r^2} + \frac{F_r}{m} \tag{22c}$$

where the radial kinematic equation has been substituted:

$$\dot{r} = w \tag{23}$$

These equations are a consistent set of equations of motion for the three generalized speeds: ω_1, ω_2, and w. The third angular velocity component remains zero at all time.

Geometrically, the constraint on ω_3 corresponds to a third rotation by the angle ψ of the quaternion frame given by the third kinematic differential equation of rotation. Expanding on the angular velocity expression in Eq. (3) to include the third rotation in ψ leaves the usual expression for a 3-2-3 rotation:

$${}^{\mathcal{I}}\boldsymbol{\omega}^{\mathcal{B}_q} = (\dot{\phi}\sin\psi - \dot{\theta}\sin\phi\cos\psi)\boldsymbol{b}_1 + (\dot{\phi}\cos\psi + \dot{\theta}\sin\phi\sin\psi)\boldsymbol{b}_2 + (\dot{\theta}\cos\phi + \dot{\psi})\boldsymbol{e}_r \tag{24}$$

Setting the third component equal to zero (the constraint $\omega_3 \equiv 0$) provides an equation for the variation of ψ,

$$\dot{\psi} = (\omega_1 \cos\psi - \omega_2 \sin\psi)\text{cotan}\,\phi \tag{25}$$

In other words, unlike the spherical frame that sets the third rotation to zero, the quaternion frame rotates about $\boldsymbol{e}_r$ to keep the equations of motion nonsingular at all angles θ and ϕ.

The kinematic relationship between the angular velocity components and the rate of change of quaternions is given by the usual relationship [11]

$$[\boldsymbol{\omega}'] = 2\boldsymbol{E}[\dot{\boldsymbol{q}}] \tag{26}$$

where $[\boldsymbol{\omega}'] = [\omega_1, \omega_2, 0, 0]^T$, and the matrix $\boldsymbol{E}$ is defined as

$$\boldsymbol{E} = \begin{pmatrix} q_4 & q_3 & -q_2 & -q_1 \\ -q_3 & q_4 & q_1 & -q_2 \\ q_2 & -q_1 & q_4 & -q_3 \\ q_1 & q_2 & q_3 & q_4 \end{pmatrix} \tag{27}$$

Equation (26) can be inverted to find the kinematic equations in which the quaternion first derivatives are written in terms of the angular velocity and quaternions:

$$\dot{q}_1 = \frac{1}{2}(q_4\omega_1 - q_3\omega_2) \tag{28a}$$

$$\dot{q}_2 = \frac{1}{2}(q_3\omega_1 + q_4\omega_2) \tag{28b}$$

$$\dot{q}_3 = \frac{1}{2}(-q_2\omega_1 + q_1\omega_2) \tag{28c}$$

$$\dot{q}_4 = \frac{1}{2}(-q_1\omega_1 - q_2\omega_2) \tag{28d}$$

In deriving the kinematic equations, the constraint $\omega_3 = 0$ has been used.

The eight first order differential equations in Eqs. (22a–22c), (23), and (28a–28d), together with the two constraints given by Eq. (17) and $\omega_3(t) = 0$ (at any t), are the new set of nonsingular equations of motion for the nine-element state variable plus mass that describes the position and velocity of the particle: $\boldsymbol{x}(t) = (r, q_1, q_2, q_3, q_4, \omega_1, \omega_2, w, m)$. These equations contain no transcendental functions: only simple algebraic operations with no singularities.

III. Testing the Equations of Motion

To verify the new quaternion-based formulation, the equations of motion have been numerically integrated in MATLAB for two simple scenarios and then compared to the results using Cartesian coordinates. The first is a two-dimensional planar trajectory in polar orbit and the second is a suboptimal three-dimensional transfer from polar orbit to GEO. In addition to verifying the new coordinates, the numerical robustness of the quaternion approach has been compared to simple Cartesian coordinates.

A. Nondimensional Units

To improve the numerical accuracy, all integrations are performed in nondimensional units. The length unit (LU) is taken equal to the GEO radius (42,157 km), whereas the initial mass of the satellite (1000 kg) represents one mass unit (MU). Specifying these two values makes it possible to derive the time unit directly from Kepler's third law. Assuming the standard gravitational parameter μ equals 1, Kepler's third law gives us a time unit (TU) of 13,716.85 s. Proper multiplicative constants to get a nondimensional thrust c_1 and characteristic constant for the satellite propulsion system c_2 can be, respectively, derived using these basic units:

$$c_1 = \frac{1}{\mathrm{MU}} \frac{\mathrm{TU}^2}{\mathrm{LU}} = 0.446 \cdot 10^2 \ \mathrm{N}^{-1} \tag{29}$$

$$c_2 = \frac{\mathrm{TU}}{\mathrm{LU}} = 0.325 \cdot 10^3 \ \mathrm{s} \cdot \mathrm{m}^{-1} \tag{30}$$

B. Two-Dimensional Case: Polar Orbit-Raising

The first case considered is a planar transfer from a polar orbit at 800 km altitude to a polar orbit at 10,000 km altitude for a small satellite of initial mass of 1000 kg, a thrust magnitude of 3 N, and a specific impulse of 2000 s. The force components F_1, F_2, and F_r with respect to $\hat{\boldsymbol{b}}_1$, $\hat{\boldsymbol{b}}_2$, and $\hat{\boldsymbol{e}}_r$ are replaced by

$$\boldsymbol{F} = \frac{T\boldsymbol{v}}{v} = T\left(\frac{r\omega_2}{v}\hat{\boldsymbol{b}}_1 - \frac{r\omega_1}{v}\hat{\boldsymbol{b}}_2 + \frac{\dot{r}}{v}\hat{\boldsymbol{e}}_r\right) \tag{31}$$

which gives the expression for a tangential thrust necessary to perform a planar transfer. Table 1 presents the final radial distance, time, mass, and fuel expenditure when integrating the equations of motion with tangential thrust using the quaternion formulation and Cartesian coordinates. The integration is performed using the explicit Runge–Kutta method of order (2, 3) with a time step of 1.58 s.

The final values of radial distance, time, and mass are exactly the same for both the quaternion-based and Cartesian formulations, verifying the approach. However, it can also be noted that the new quaternion-based formulation is less sensitive to numerical error. In fact, when performing the integration for different solving algorithms keeping both the relative and absolute error tolerances at the relatively relaxed values of 10^{-3} and 10^{-6}, respectively, the final radial distance found is significantly more sensitive to the algorithm choice for the Cartesian formulation than for the quaternion-based. The results can be seen in Table 2, where the different algorithms used are denoted by numerical differentiation formulas (NDFs), Adams–Bashforth–Moulton (ABM), Runge–Kutta (2, 3) (RK23), the modified Rosenbrock formula of second order (MR2), the trapezoidal rule (TR), and the trapezoidal rule plus backward differentiation formulas of the second order (TR-BDF2). It takes a significant reduction in error tolerances to make the Cartesian formulation behave as stably as the quaternion one. Also, although it was possible to use an explicit Runge–Kutta (4, 5) formula to integrate the problem formulated using quaternions with the relative and absolute error tolerances at 10^{-3} and 10^{-6}, respectively, the same approach using the Cartesian formulation was not able to meet integration tolerances without reducing the step size below the smallest value allowed. This highlights the challenge of using Cartesian coordinates and one of the motivations for the quaternion formulation.

C. Three-Dimensional Case: Orbital Transfer from a Polar Orbit to a Geostationary Orbit

In this section, considered as a test case is the transfer of a large satellite of mass 3500 kg from a polar orbit at 10,000 km altitude to GEO. The spacecraft uses four BPT-4000 thrusters of 0.29 N each with a specific impulse of 1788 s. At any instant of time t, we denote by $\boldsymbol{r}(t)$, $\boldsymbol{v}(t)$, and $\boldsymbol{h}(t)$ the radius, velocity, and angular momentum vectors of the satellite. To perform the transfer, it is assumed that the thrust is always constrained to be in the plane defined by the velocity vector $\boldsymbol{v}(t)$ and the angular momentum vector $\boldsymbol{h}(t)$. Let the thrust vector have magnitude $T(t) = T_{\max}$ at all times. Its direction is given by the unit vector $\boldsymbol{e}_T$, which varies with time. This direction is defined by the angle $\beta(t)$ with respect to the velocity vector $\boldsymbol{v}(t)$. Let $v_\perp(t)$ be the component of the velocity vector perpendicular to the equatorial plane. Based on the sign of this component of velocity, the following thrust profile for the satellite orbit-raising maneuver is considered:

$$\boldsymbol{T}(t) = \begin{cases} \cos\beta_0 \frac{\boldsymbol{v}(t)}{v(t)} + \sin\beta_0 \frac{\boldsymbol{h}(t)}{h(t)}, & \text{if } v_\perp < 0 \\ \cos\beta_0 \frac{\boldsymbol{v}(t)}{v(t)} - \sin\beta_0 \frac{\boldsymbol{h}(t)}{h(t)}, & \text{if } v_\perp > 0 \\ 0 & \text{if } v_\perp = 0 \end{cases} \tag{32}$$

The assumption that there exists a constant $\beta_0 \in [0 \ \mathrm{deg}, 90 \ \mathrm{deg}]$ such that the satellite attains the radius and the inclination of GEO in a finite time is introduced. Using the thrust profile in Eq. (32) and the satellite specifications already mentioned, the quaternion-based and Cartesian sets of equations are integrated in MATLAB using the Adams–Bashforth–Moulton method. The results are shown in Table 3.

Table 3 shows perfect accordance between the two sets of equations and provides an approximate upper bound for transfer time and fuel expenditure to transfer a satellite from a medium polar orbit to GEO. In Fig. 2, the altitude z is plotted versus x, showing how z increases and then decreases during the transfer. The plot is the same for both sets of equations, and the radius increases at a more rapid rate than the inclination decreases, so the amplitude of z increases during the initial part of the transfer but eventually decays to zero.

As a further test of the equations of motion, the trajectory integration was repeated with varying thrust, initial mass, and thrust direction. The results are tabulated in Tables 4–6. In this test, one parameter at time was changed while keeping all the others fixed. Note

Table 1 2-D orbit-raising test

Coordinates	r_F, km	t_F, d	m_F, kg	Fuel expenditure, kg
Quaternions	10,053.4	9.15	879.0	121.0
Cartesian	10,053.4	9.15	879.0	121.0

Table 2 Final radius for the quaternion-based and Cartesian formulation for different numerical integration techniques

Solver	NDFs	ABM	RK23	MR2	TR	TR-BDF2
Quaternions	0.3892	0.3895	0.3896	0.3898	0.3898	0.3898
Cartesian	0.5424	0.3483	0.4363	0.4357	0.4165	0.3811

Table 3 3-D orbital transfer from a polar orbit to near GEO

Coordinates	r_F, km	t_F, d	m_F, kg	Fuel expenditure, kg
Quaternions	42,164	263.65	1993.0	1507.0
Cartesian	42,164	263.65	1993.0	1507.0

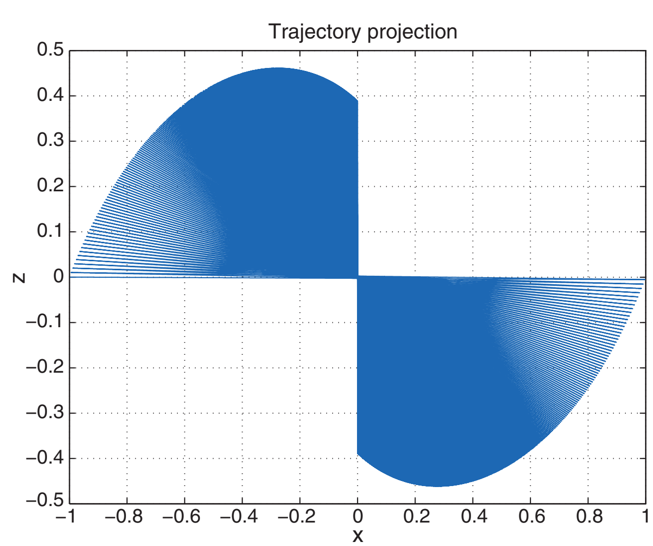

Fig. 2 Trajectory projection on xz plane.

Table 4 3-D orbital transfer from a polar orbit to GEO: thrust

Thrust, N	r_F (GEO = 1)	t_F, d	m_F, kg	Fuel expenditure, kg
1	1.0001	292.98	1810.9	1689.1
2	1.0018	170.60	2516.5	983.5
3	0.9976	119.49	2811.1	688.9

Table 5 3-D orbital transfer from a polar orbit to GEO: initial mass

Initial mass, kg	r_F (GEO = 1)	t_F, d	m_F, kg	Fuel expenditure, kg
4000	1.0004	301.39	2277.3	1722.7
2000	0.9977	150.44	1140.1	859.9
1500	1.0031	113.20	853.0	647.0

Table 6 3-D orbital transfer from a polar orbit to GEO: thrust angle

Thrust angle, deg	r_F (GEO = 1)	t_F, d	m_F, kg	z_F (GEO = 1)
80	0.9277	266.67	1975.7	0.0008
78	1.1090	259.87	2014.6	0.0003
76	1.3273	253.29	2052.2	0.0027

that, when the thrust angle changes, the spacecraft reaches the equatorial plane at a different altitude than GEO, which supports the assumption that there exists one constant thrust direction such that the satellite attains the radius and the inclination of GEO in a finite time.

When changing the thrust value, the specific impulse changes as well while keeping constant the engine mass flow rate. An increase in thrust correctly reduces the transfer time. Although it might appear from Tables 4–6 that less fuel is required when increasing the thrust, this conclusion would be incorrect because of the assumption on the mass flow rate (assumed to be constant). In the case of a change of the initial mass of the spacecraft, a lighter satellite requires, as expected, less time to transfer to near GEO. Finally, the scenario was examined in which the constant thrust angle ($\beta_0 = 79.15$ deg in the first case, shown in Table 3), is modified while keeping all the other parameters unchanged. It can be observed that an increase in the thrust angle, which means a larger out-of-plane thrust component, translates into a lower final radius compared to the one reached when applying less out-of-plane thrust. This is expected because of the way in which the thrust is distributed among in-plane and out-of-plane components. When a bigger fraction of thrust is used for the plane-change maneuver instead of the orbit raising, then the final radius is less than GEO. Note also that the value $\beta_0 = 79.15$ deg is the one that brings the satellite exactly to GEO, getting closer to the equatorial plane than higher or larger values of thrust angle.

IV. Conclusions

In this Note, it was shown how a nonsingular formulation of the low-thrust orbit-raising problem can be obtained using quaternions instead of the spherical angle coordinates. A quaternion-based formulation has the twofold advantage of avoiding any singularity in the equations of motion and, at the same time, keeping the numerical implementation more robust. The new formulation was verified on two simple orbit-raising maneuvers by comparing to Cartesian coordinates. The first case to be considered was the one of a simple coplanar transfer of a small satellite from 800 to 10,000 km altitude at 90 deg inclination and applying a 3 N tangential thrust. The results show how the new formulation remains consistent, apart from an integration error, with that obtained when performing the integration in Cartesian coordinates. The second scenario was a plane-change maneuver of a large satellite from a polar orbit at 10,000 km altitude to geostationary Earth orbit applying a total thrust of 1.16 N. The new quaternion-based formulation proved again to be in accordance with the reference model. As further testing, the equations' behavior was analyzed when one parameter at time was changed in the problem, showing the expected trend in the integration output.

The performed tests show the potential of the new nonsingular quaternion-based formulation applied to the all-electric orbit raising of a GEO satellite. Given its generality, the same formulation can be used to solve any low-thrust problem. At the same time, the absence of any singularity allows for the investigation of high-inclination injection orbits to transfer to GEO. Future work will include the inclusion of the new equations of motion into an optimization scheme that minimizes both transfer time and radiation exposure of the satellite, as well as a systematic application of the formulation to the problem of high-inclination injection orbits.

Acknowledgments

This work was performed under an agreement with Société Européenne des Satellites (SES) Engineering dated April 1, 2011. We thank Philippe Francken and Stan Russo of SES for their help and suggestions.

References

[1] de Selding, P. B., "SES Chief Prefers Modular Ariane 6 for Launch Flexibility," *Space News*, March 2012, available online at http://www.spacenews.com/article/ses-chief-prefers-modular-ariane-6-launch-flexibility.

[2] Griffiths, S., "The Record-Breaking NASA Rocket That's Run Non-Stop for Five Years and Could Be Used in Deep Space Science Missions of the Future," *Daily Mail*, June 2013, available online at http://www.dailymail.co.uk/sciencetech/article-2349785/The-record-breaking-Nasa-rocket-thats-run-non-stop-years-used-deep-space-science-missions-future.html.

[3] Dutta, A., Libraro, P., Kasdin, N. J., and Choueiri, E. Y., "A Direct Optimization Based Tool to Determine Orbit-Raising Trajectories to GEO for All-Electric Telecommunication Satellites," *AIAA/AAS Astrodynamics Specialist Conference*, AIAA Paper 2012-4589, Aug. 2012.
doi:10.2514/6.2012-4589

[4] Dutta, A., Libraro, P., Kasdin, N. J., and Choueiri, E. Y., "Minimizing Total Radiation Fluence During Time-Constrained Electric Orbit-Raising," *International Symposium on Space Flight Dynamics*, Pasadena, CA, 2012, available online at http://issfd.org/ISSFD_2012/ISSFD23_ODY_4.pdf.

[5] Dutta, A., Libraro, P., Kasdin, N. J., and Choueiri, E. Y., "Satellite Power Subsystem Requirements for Time-Constrained Electric Orbit-Raising with Minimal Radiation Impact," *AAS Space Flight Mechanics Meeting*, American Astronautical Soc. Paper 2013-256, Kauai, HI, Feb. 2013.

[6] Conway, B. A., *Spacecraft Trajectory Optimization*, Cambridge Univ. Press, New York, 2010, pp. 112–136.

[7] Gurfil, P., "Euler Parameters as Nonsingular Orbital Elements in Near-Equatorial Orbits," *Journal of Guidance, Control, and Dynamics*, Vol. 28, No. 5, Sept.–Oct. 2005, pp. 1079–1084.
doi:10.2414/1.14760

[8] Hudson, J. S., and Scheeres, D. J., "Reduction of Low-Thrust Continuous Controls for Trajectory Dynamics," *Journal of Guidance, Control, and Dynamics*, Vol. 32, No. 3, May–June 2009, pp. 780–787.
doi:10.2514/1.40619

[9] Gaylor, D. E., "Analysis of Low Thrust Orbit Transfers Using the Lagrange Planetary Equations," *Lightsey Research Group at University of Texas Center for Space Research*, Austin, TX, 2000, available online at http://www.researchgate.net/publication/253281043_ANALYSIS_OF_LOW_THRUST_ORBIT_TRANSFERS_USING_THE_LAGRANGE_PLANETARY_EQUATIONS.

[10] Wie, B., *Space Vehicle Dynamics and Control*, 2nd ed., AIAA Education Series, AIAA, Reston, VA, 2008, pp. 403–477.

[11] Kane, T. R., Likins, P. W., and Levinson, D. A., *Spacecraft Dynamics*, McGraw–Hill, New York, 1983, pp. 12–16, 58–62, 159–246.

[12] Pisacane, V. L., and Moore, R. C., *Fundamentals of Space Systems*, Oxford Univ. Press, Oxford, England, U.K., 1994, pp. 260–318.

[13] Wertz, J. R., *Spacecraft Attitude Determination and Control*, D. Reidel Publishing, Dordrecht, The Netherlands, 1978, pp. 510–540.

[14] Wie, B., and Barba, P. M., "Quaternion Feedback for Spacecraft Large Angle Maneuvers," *Journal of Guidance, Control, and Dynamics*, Vol. 8, No. 3, May–June 1985, pp. 360–365.
doi:10.2514/3.19988

[15] Davailus, G. P., and Newman, B. A., "The Application of Quaternion Algebra to Gyroscopic Motion, Navigation and Guidance," *AIAA Guidance, Navigation and Control Conference and Exhibit*, AIAA Paper 2005-5945, Aug. 2005. doi:10.2514/6.2006-6657

[16] Kasdin, N. J., and Paley, D. A., *Engineering Dynamics: A Comprehensive Introduction*, Princeton Univ. Press, Princeton, NJ, 2011, pp. 413–420.

[17] Boyce, W. E., and DiPrima, R. C., *Elementary Differential Equations and Boundary Value Problems*, 10th ed., Wiley, New York, 2012, pp. 186–192.